Study on preparation and structure of chrysanthemum-shaped micron calcium carbonate based on inverse microemulsion

Tiaobin Zhao[1], *Chao Xu*[1], *Yitong Ma*[1], *Yiwen Zeng*[2], *Nong Wang*[1] ✉

[1]*School of Chemical and Biological Engineering, Lanzhou Jiaotong University, Lanzhou 730070, People's Republic of China*
[2]*College of Materials and Chemical Engineering, Hezhou University, Hezhou, Guangxi, 542899, People's Republic of China*
✉ *E-mail: wangnong07@163.com*

Published in Micro & Nano Letters; Received on 22nd June 2020; Revised on 28th September 2020; Accepted on 12th October 2020

In this Letter, new chrysanthemum-shaped micrometre calcium carbonate was prepared by using $CaCl_2$ aqueous solution + NH_3H_2O + CTAB + n-butanol + n-hexane inverse microemulsion system. Scanning electron microscope, X-ray powder diffraction, and Fourier transform infrared spectroscopy were used to characterise the morphology and structure of the micron calcium carbonate. Further, the formation mechanism of chrysanthemum-shaped micron calcium carbonate was discussed.

1. Introduction: In nature, calcium carbonate ($CaCO_3$) exists in ores, such as limestone, calcite, and chalk, as well as in clam, oyster and other shells [1–3]. According to the crystal structure, it is mainly divided into aragonite, calcite, and vaterite [4, 5]. Micro and nano $CaCO_3$s are important inorganic chemical products. They are non-toxic, odourless, and fine white powder produced by mechanical pulverising or carbonisation method. The powders are usually slightly alkaline and insoluble in water, easily absorbs moisture, and have stable chemical properties. As fillers and reinforcing agents, they are widely used in the rubber, plastics, building materials, paper, coatings, inks, food, feed, toothpaste, cosmetics [6–8], etc. $CaCO_3$ properties and applications, mainly depend upon its morphology, structure, particle size, and chemical purity of a crystal. Among them, the spindle-shaped $CaCO_3$ [9] is similar to that of microfibres which imparts excellent properties such as bulkiness, writing, opacity, smoothness, and printability to paper. Cubic $CaCO_3$ [10] exhibits high whiteness and opacity in paper and improves the electrical properties, flame retardancy, impact resistance, and processing characteristics of plastic products. It can replace white carbon black in rubber filler, makes the product surface bright, higher elongation, flex index, and has a strong anti-cracking performance. Spherical $CaCO_3$ [11] has good opacity and the ability to absorb ink and can be added to lubricating oil to greatly improve its lubricity. Flake $CaCO_3$ [12] has super optical properties and printing properties. When used for coated paper coating pigments, it has good fluidity and dispersibility. It shows better gloss and smoothness than ordinary spindle $CaCO_3$, so it can partially replace flake kaolin which is increasingly scarce. Zhang *et al.* [13] and Pryputniewicz *et al.* [14] studied the influence of particle size on the toughening properties. They found that micro–nano composite $CaCO_3$ can improve the toughness of a material. So $CaCO_3$ particles with special structure and morphology may have some special purposes. Accordingly, with the increasing demand for the comprehensive performance of $CaCO_3$ in various industries, the researches on $CaCO_3$ are moving towards ultra-fine and functionalisation. Many research scholars are committed to artificially regulating the morphology and structure of $CaCO_3$ through various technical means [15]. Among them, the inverse microemulsion method has become one of the research hotspots in recent years [16–19]. The inverse microemulsion is a water-in-oil dispersion system mainly composed of oil, aqueous, co-surfactants, and surfactants. Due to the special properties of surfactants [20–26], they can help to form nano-scale microreactors in microemulsion [27]. As an emerging preparation method, it has many advantages, such as the equipment and preparation process are simple, the size of the nanoparticles can be controlled by adjusting the size of the reactor. The instability (agglomeration, oxidation, etc.) of the nanoparticles that may be caused during other preparation methods is well avoided, and the particles synthesised by this method have small size and good dispersibility.

In this Letter, we choose cyclohexane as the oil phase, the surfactant and co-surfactant were CTAB and n-butanol, respectively, the CO_2 was introduced into the mixture solution, and the reaction temperature was kept at room temperature. $CaCO_3$ particles were synthesised by using the mixture solution of calcium chloride and ammonia water as a water phase to form a precipitate in the microemulsion [28, 29]. The novelty chrysanthemum-shaped micron $CaCO_3$ was successfully prepared by this method, and this research would provide some guidance for the study of different shapes and crystals of $CaCO_3$.

2. Materials and methods

2.1. Materials: Chemicals used in this study were from different sources: calcium chloride and ammonia were purchased from Tianjin Damao Chemical Factory, China. Cetyltrimethylammonium bromide (CTAB) and cyclohexane were purchased from Shandong Shuangshuang Chemical Factory, China. N-butyl alcohol was purchased from Shanghai Zhongqin Chemical Factory, China. Distilled water was produced by our laboratory. All the chemicals were analytically graded and used without further purification. All aqueous solutions were prepared using distilled water.

2.2. Synthesis of $CaCO_3$ with different morphologies: Calcium chloride and ammonia were mixed and diluted in water. Then mixed the aqueous solution, cyclohexane, n-butanol, and CTAB to prepare a stable inverse microemulsion. The volume ratio of the aqueous solution, oil, co-surfactant, and surfactant is 2: 50: 15: 8. The CO_2 gas was introduced into the microemulsion at the rate of 300 ml/min. All the experiments are carried out at room temperature.

At the beginning of the reaction, the microemulsion system was clear and transparent. With the continuous penetration of CO_2, the microemulsion began to become turbid. During the precipitation, the solution was continuously stirred at a constant rate of 650 r/min. The reaction was not stopped until the pH value dropped to 7. After ageing for 24 h, the final precipitation was centrifuged at 3000 r/min for 5 min, and then the solid was redispersed in ethyl alcohol. This process was repeated three times. After the

last centrifugation, the particles were dried in the oven at 70°C for 24 h.

Other micron $CaCO_3$ were also prepared under the same reverse microemulsion method except that the stirring speed and the volume ratio of water, oil, co-surfactant, and surfactant. The stirring speed is 0, 500, and 1000 r/min, respectively. The volume ratio of water, oil, co-surfactant, and surfactant is 4: 50: 15: 8.

2.3. Equipment and characterisation: The size and morphology of the $CaCO_3$ powder samples were analysed by scanning electron microscopy (SEM; JSM-6100, JEOL Ltd, Japan). Infrared spectroscopy was recorded by a Fourier transform infrared spectrometer (FTIR; EXUS–470, Nicolet, Japan). The crystal structure types were analysed by powder X-ray diffraction (XRD; RINT-1000, Rigaku, Japan). All the glassware and storage bottles were immersed in hydrochloric acid overnight and then rinsed thoroughly with distilled water.

3. Results and discussion

3.1. Morphology: In the process of experiment, we found that different preparation methods, even a small change in the type and amount of additives or a slight change in reaction conditions would cause a huge change in crystal morphology and particle shape [30–33].

It can be seen in Fig. 1 that when $CaCO_3$ prepared without stirring, the shape of the $CaCO_3$ particles is cube-like. In Fig. 2, we found that the micron $CaCO_3$ have both cube-like shape and sphere-like shape particles when the stirring speed is 500 r/min. It can be found in Fig. 3 that when the stirring speed is 1000 r/min, cube-like

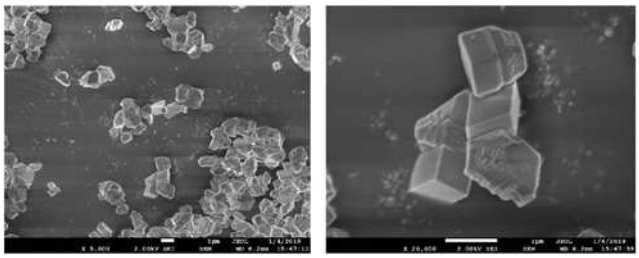

Fig. 1 *SEM image of $CaCO_3$ prepared without stirring*

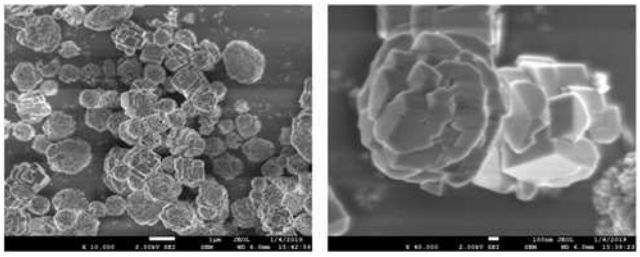

Fig. 2 *SEM image of $CaCO_3$ prepared at a stirring speed of 500 r/min*

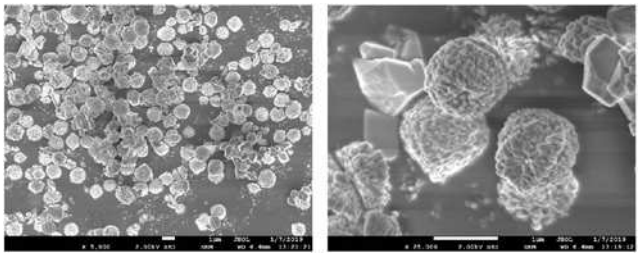

Fig. 3 *SEM image of $CaCO_3$ prepared at a stirring speed of 1000 r/min*

$CaCO_3$ and sphere-like $CaCO_3$ particles are also obtained, it seems that with the increases of stirring speed, there are more sphere-like shape $CaCO_3$ particles obtained, but there are not special morphology of $CaCO_3$ was produced until we change the volume ratio of water, oil, co-surfactant, and surfactant to 2: 50: 15: 8, and change the stirring speed to 650 r/min. These can be found in Fig. 4 that the chrysanthemum-shaped micrometre $CaCO_3$ was produced, and the surface of the chrysanthemum-like micrometre $CaCO_3$ has multiple layers folds, it looks like a blooming chrysanthemum, and they have a uniform shape, good dispersion, and good stability.

3.2. Structure and crystal type: Fig. 5 is the standard X-ray diffraction pattern of vaterite and calcite. The observed peaks in Fig. 5 are indexed as vaterite and calcite; in agreement with PDF#33-0268 and PDF#47-1743. Comparing with aragonite $CaCO_3$ PDF#41-1475 card, it is found that its standard spectrum, mainly has diffraction peaks at 21.07°, 26.22°, 31.13°, 33.15°, 37.90°, 41.22°, 45.86°, and 50.25°. Since there is no main diffraction peak of aragonite $CaCO_3$ in the XRD diagram of prepared $CaCO_3$, so aragonite $CaCO_3$ was not discussed in this Letter.

Fig. 6*a* shows the XRD pattern of cube-like $CaCO_3$. Diffraction peaks appearing at 2θ of 23.03°, 29.34°, 35.81°, 39.25°, 43.03°, 47.29°, and 48.36° correspond to (012), (104), (110), (113), (202), (018), and (116) crystal planes of the calcite $CaCO_3$. This is the same as the standard X-ray diffraction pattern for calcite (as shown in Fig. 5), indicating that the prepared micron $CaCO_3$ crystal form is calcite. However, comparing Figs. 6*b–d* with the standard XRD pattern of vaterite and calcite (Fig. 5), we found this $CaCO_3$ has both calcite and vaterite while stirring. Since the volume ratio of water, oil, co-surfactant, and surfactant for preparing chrysanthemum-shaped $CaCO_3$ is different from $CaCO_3$ which have both cube-like shape and sphere-like shape particles. So the formation of chrysanthemum-shaped micron $CaCO_3$ is also related to the other reaction condition, such as crystallisation temperature, the molar ratio [34] of water and surfactant, etc. [35–40].

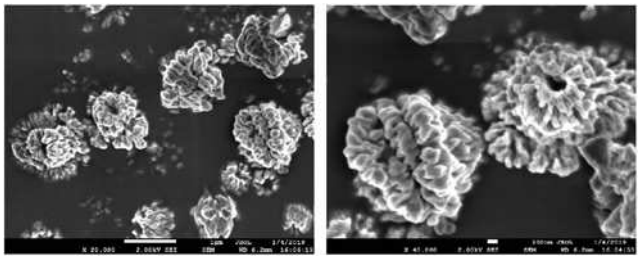

Fig. 4 *SEM image of chrysanthemum-shaped micron $CaCO_3$ (stirring speed is 650 r/min)*

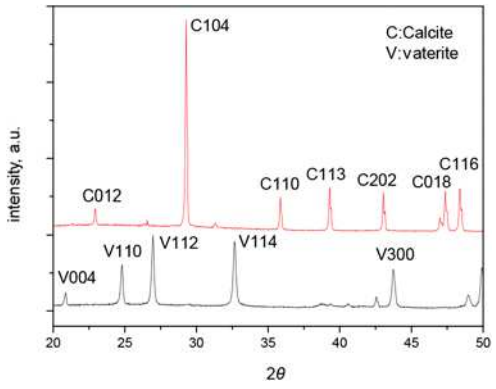

Fig. 5 *Standard XRD pattern of vaterite and calcite*

doi: 10.1049/mnl.2020.0349

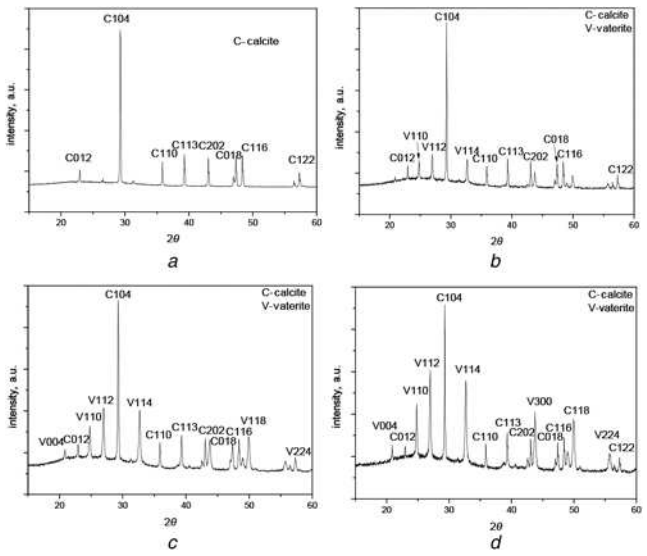

Fig. 6 *XRD pattern of $CaCO_3$*
a Without stirring
b Stirring speed is 500 r/min
c Stirring speed is 650 r/min (chrysanthemum-shaped) and
d Stirring speed is 1000 r/min)

To compare the relative content of vaterite phase and calcite phase in $CaCO_3$, the highest diffraction peaks of (104) crystal plane of calcite and (112) crystal plane of vaterite were selected as the characteristic peaks of calcite and vaterite (expressed as C104 and V112, respectively, the same below). By comparing the relative heights of peak V112 and C104 in the XRD diagrams of Figs. 6*a–d*, the relative contents of calcite and vaterite can be obtained approximately, the larger the ratio, the higher the relative content of vaterite. It is found that when the stirring speed is 0, 500, 650, and 1000 r/min, respectively, the ratio of the peak height is roughly 0, 0.15, 0.31, and 0.55. The ratio of peak height increases as the stirring speed increases. Therefore, it shows that increasing the stirring speed is beneficial to the production of vaterite phase $CaCO_3$. Almost all calcite phase $CaCO_3$ is generated without stirring. This may be because once $CaCO_3$ form they tend to cluster together without stirring, and two phases of water and oil will be easily formed after demulsification that makes the larger calcite phase $CaCO_3$ particles are formed easily. Stirring is beneficial to the dispersion of the water phase in the oil phase. The faster the stirring speed, the more favourable is the dispersion of the surfactant in the oil-water interface, which is helpful to maintain the presence of the microemulsion phase, making $CaCO_3$ easily form more small nanoscale particles in the micro pool. The small particles, which in turn aggregate, make the system form more vaterite phase $CaCO_3$. On the other hand, although calcite is more stable than vaterite, during the growth of $CaCO_3$ crystals in the reverse microemulsion system, vaterite is easier to form than calcite, so under high-speed stirring, calcium ions and carbonate ions in the solution have been greatly disturbed, making it difficult to enter the determined lattice position of calcite, on the contrary, it is easier to form vaterite $CaCO_3$.

The infrared spectra of chrysanthemum-shaped and other $CaCO_3$ prepared at different stirring speeds were shown in Fig. 7. The wavenumbers range change from 200 to 2000 cm^{-1}. From Fig. 7*a*, it can be seen that the broad peak of cube-like $CaCO_3$ at 1393 cm^{-1} is the C–O asymmetric stretching vibration peak of calcite crystal and the peak at 874 cm^{-1} is attributed to the out-of-plane bending vibration of the carbon–oxygen bond of calcite crystal, the peak at 711 cm^{-1} is attributed to the in-plane deformation vibration of the carbon–oxygen bond of calcite crystal [41–43]. Figs. 7*b–d* show the characteristic peaks similar

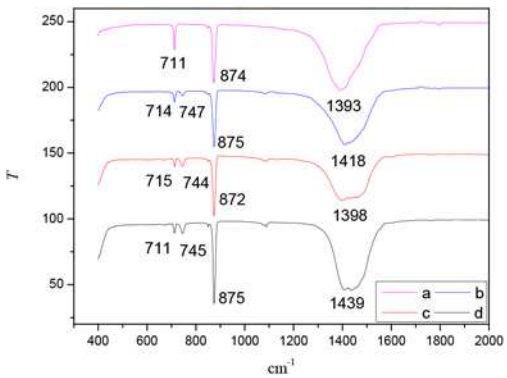

Fig. 7 *FTIR of $CaCO_3$*
a Without stirring
b Stirring speed is 500 r/min
c Stirring speed is 650 r/min (chrysanthemum-shaped) and
d Stirring speed is 1000 r/min

to Fig. 7*a*, except the peak at 747 cm^{-1} which is the characteristic absorption peak of vaterite. These results show that it is beneficial to form the vaterite phase $CaCO_3$ after stirring.

3.3. Formation mechanism of chrysanthemum-shaped micron $CaCO_3$: We believe that the formation of chrysanthemum-shaped micron $CaCO_3$ may be firstly due to that the small water pools (we also call it droplets) gather around the carbon dioxide bubbles when carbon dioxide is bubbled into the microemulsion, and the carbon dioxide penetrated the small water pools combines with Ca^{2+} to form nano $CaCO_3$ which has a similar size of the droplet. With continuous injection CO_2 continuously reacts with the surrounding microwater pools to form layers of nano $CaCO_3$ accumulations, just like the layered leaves of chrysanthemum, and the centre of the carbon dioxide bubble forms the stamens of chrysanthemum, and because of other factors, such as stirring, viscosity, temperature, pressure of carbon dioxide bubbles [44–48], etc. chrysanthemum-shaped micro–nano $CaCO_3$ was finally formed. The formation principle of chrysanthemum-shaped $CaCO_3$ is shown in Fig. 8.

3.4. Size of small water pool and nano $CaCO_3$: Assuming that the droplets of microemulsion have the same size, and the surfactant is evenly dispersed on the contact surface of the droplet, we can estimate the particle size of the droplet (R_m), and its radius expression formula is [49]

$$R_m = \frac{3V_h}{A_s}\omega_0 \tag{1}$$

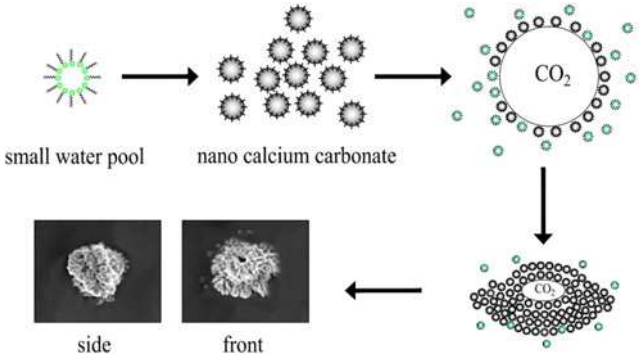

Fig. 8 *Schematic illustration of chrysanthemum-shaped $CaCO_3$ formation*

where V_h is the volume of a water molecule (3.0×10^{-29} m^3), ω_0 is the mole ratio of water to surfactant content, and A_s is the area per molecule of surfactant at the oil/water interface. In the case of CTAB, A_s was previously suggested to be 0.64 nm^2 by Warr *et al.* [50].

Formula (1) can be used to calculate the size of the small water pool in the microemulsion. However, due to the presence of n-butanol, which was used as a co-surfactant in the microemulsion. The co-surfactant can be inserted into the structure of the reverse micelle to increase the size of the reverse micelle. So we assume that there is some amount of n-butanol dissolved in the water phase, then the particle size R_m^1 of the droplet can be estimated, the formula for calculating its radius is

$$R_m^1 = \frac{3(n_h V_h + n_{alc} V_{alc})}{A_s n_{CTAB}} \quad (2)$$

where n_h is the amount of substance in the water phase, n_{alc} is the amount of n-butanol dissolved in water, V_{alc} is the volume of an n-butanol molecule (1.52×10^{-28} m^3), n_{CTAB} is the amount of CTAB substance. According to formula (2), we can calculate the radius of the droplet in the microemulsion, it is $R_m^1 = 1.52$ nm. According to the study of Wang Nong's group [16], the size between experimental result and theoretical calculation values according to the CTAB micelle droplet in a microemulsion is different, there is a correction factor k between the experimental value and the theoretical value, which is about $k = 10.53 \pm 0.56$, therefore, the theoretical calculation value in our system is $D_1 = 31.98$ nm.

Due to CTAB is distributed on the oil–water interface, and the generated $CaCO_3$ will be coated with a layer of CTAB, so the chain length of CTAB needs to be considered. The C–C bond length of CTAB is about 1.5 Å, and bond angle of C–C–C is 110°. The calculated chain length of CTAB is about 2.35 nm. Therefore, the diameter of $CaCO_3$ calculated from the droplet by considering the chain length of CTAB is 36.68 nm.

The lower left of Fig. 9 is a lateral electron microscope picture of chrysanthemum-shaped $CaCO_3$, because the spherical papillae in the right side of the picture are more clearly, so they were considered as nano $CaCO_3$ which accumulate to form the chrysanthemum-shaped micron $CaCO_3$, some of them were selected for measurement the size of papillae. The diameter of these papillae are $D_{a1} = 47$ nm, $D_{a2} = 43$ nm, and $D_{a3} = 40$ nm. The average particle size is about $D_a = 43$ nm, this result is almost the same with the $CaCO_3$ particle size obtained from the calculation.

We also use the same method to calculate the papillary diameter of the $CaCO_3$ prepared at a stirring speed of 1000 r/min, it is $D_2 = 53.60$ nm, the diameter of the papilla on the surface of $CaCO_3$ measured in the experiment is shown in Fig. 10, which is

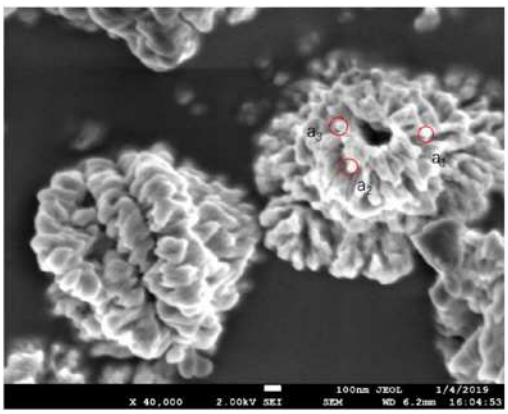

Fig. 9 *Enlarged view of chrysanthemum-shaped $CaCO_3$*

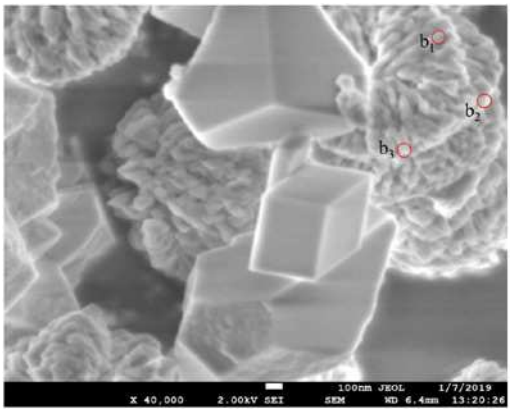

Fig. 10 *Enlarged view of $CaCO_3$ prepared at a stirring speed of 1000 r/min*

$D_{b1} = 50$ nm, $D_{b2} = 50$ nm, $D_{b3} = 52$ nm, and the average diameter is about $D_b = 50$ nm. So we obtained a similar result that the size of the $CaCO_3$ particle calculated is almost the same with the experiment. Due to the surfactant for preparing $CaCO_3$ at stirring speed of 1000 r/min is less than for preparing chrysanthemum-shaped $CaCO_3$, so it has a bigger mole ratio of water to surfactant content, resulting in bigger droplet and particles size.

4. Conclusion: Chrysanthemum-shaped micron $CaCO_3$ was prepared by an inverse microemulsion system. We found that the stirring speed has a great influence on the crystal form of $CaCO_3$. In the process of experiment, without stirring, calcite $CaCO_3$ was mainly formed, and relatively more vaterite is formed after the stirring speed becomes higher. Then chrysanthemum-shaped $CaCO_3$ is produced by many factors combined such as reducing the amount of water, viscosity increases, and carbon dioxide bubbles, etc. This research will provide a reference for preparing a new type of micro/nano $CaCO_3$ with special morphology and structure.

5. Acknowledgments: This work was supported by the Key Technology and Industrial Application Demonstration Project of High Quality and High Purity Nano Calcium Carbonate of Guangxi Province (grant no. 17202030-2), the Innovation Fund of Small and Medium-sized Enterprises of Gansu Province (grant no. 1407GCCA013).

6 References

[1] Porter S.M.: 'Seawater chemistry and early carbonate biomineralization', *Science*, 2007, **316**, (5829), p. 1302
[2] Stupp S.I., Braun P. V.: 'Molecular manipulation of microstructures: biomaterials, ceramics, and semiconductors', *Science*, 1997, **277**, (5330), pp. 1242–1248
[3] Mann R.: 'Biomineralization: principles and concepts in bioinorganic materials chemistry', *Cryst. Growth Des.*, 2002, **4**, (2), pp. 675–676
[4] Xing X., Sun R., Wang S.: 'Characteristics of calcium carbonate crystal structure and size distribution in solution under the electromagnetic field', *Adv. Mater. Res.*, 2011, **284–286**, pp. 2136–2140
[5] Xu B., Poduska K.M.: 'Linking crystal structure with temperature-sensitive vibrational modes in calcium carbonate minerals', *Phys. Chem. Chem. Phys.*, 2014, **16**, (33), pp. 17634–17639
[6] De Oliveira I.R., Amico S.C., De Lima A.G.B., *ET AL.*: 'Application of calcium carbonate in resin transfer molding process: an experimental investigation', *Materwiss. Werksttech.*, 2015, **46**, (1), pp. 24–32
[7] De Oliveira I.R., Amico S.C., Barcella R., *ET AL.*: 'Application of calcium carbonate in resin transfer molding process', *Defect Diffus. Forum*, 2014, **353**, pp. 39–43
[8] Qiu H.H., Luo K.B., Li H.P.: 'Progress on preparation and application of calcium carbonate whisker', *Adv. Mater. Res.*, 2015, **1094**, pp. 113–117
[9] Jiang J., Xu D., Zhang Y., *ET AL.*: 'From nano-cubic particle to micro-spindle aggregation: the control of long chain fatty acid on the

doi: 10.1049/mnl.2020.0349

morphology of calcium carbonate', *Powder Technol.*, 2015, **270**, (Part A), pp. 387–392
[10] Saulat H., Cao M., Khan M.M., *ET AL.*: 'Preparation and applications of calcium carbonate whisker with a special focus on construction materials', *Constr. Build. Mater.*, 2020, **236**, p. 117613
[11] Gorna K., Hund M., Vučak M., *ET AL.*: 'Amorphous calcium carbonate in form of spherical nanosized particles and its application as fillers for polymers', *Mater. Sci. Eng. A*, 2008, **477**, (1–2), pp. 217–225
[12] Tu Chao S.: 'Application of flake calcium carbonate in fine paper', *Pap. Chem.*, 2001, **16**, (9), pp. 123–126
[13] Zhang J., Li L., Zhou N.L., *ET AL.*: 'Effects of mechanical property of PP filled with nano/micron $CaCo_3$ complex sizes fillers', Proc. National Polymer Materials Science and Engineering Symp. (in Chinese), 2006, pp. 553–556
[14] Pryputniewicz R.J., Furlong C., Pryputniewicz E.J.: 'Analytical and experimental characterization of an optical MEMS device', *Proc. SPIE – Int. Soc. Opt. Eng.*, 2003, **5288**, pp. 774–779
[15] Hartman P.P.W.G.: 'On the relations between structure and morphology of crystals III', *Acta Crystallogr.*, 1995, **8**, (9), pp. 528–529
[16] Wang N., Wang X., Yang L., *ET AL.*: 'Morphology and size control of nanocalcium carbonate crystallised in reverse micelle system with cationic surfactant cetyltrimethylammonium bromide', *Micro Nano Lett.*, 2013, **8**, (2), pp. 94–98
[17] Naka K., Chujo Y.: 'Control of crystal nucleation and growth of calcium carbonate by synthetic substrates', *Chem. Mater.*, 2001, **13**, (10), pp. 3245–3259
[18] Lu H.B., Ma C.L., Cui H., *ET AL.*: 'Controlled crystallization of calcium phosphate under stearic acid monolayers', *J. Cryst. Growth*, 1995, **155**, (1–2), pp. 120–125
[19] Wang N., Meng Q.L.: 'Study of the influence between barium ions and calcium ions on morphology and size of coprecipitation in microemulsion', *Surf. Rev. Lett.*, 2015, **22**, (3), pp. 1–10
[20] Wang N., Zhao M.: 'Study on thermodynamics and kinetics of association interactions between malachite green and OP-10 in aqueous solutions', *J. Dispersion Sci. Technol.*, 2016, **37**, (2), pp. 190–195
[21] Tohse H., Saruwatari K., Kogure T., *ET AL.*: 'Control of polymorphism and morphology of calcium carbonate crystals by a matrix protein aggregate in fish otoliths', *Cryst. Growth Des.*, 2009, **9**, (11), pp. 4897–4901
[22] Wang N., Su C., Xiao S.: 'Interaction of phenol red with cetyltrimethylammonium bromide in aqueous solution', *Color. Technol.*, 2015, **131**, (6), pp. 434–438
[23] Guo J., Wang Z., Jing J., *ET AL.*: 'Interaction between Coomassie Brilliant Blue G250 and octylphenol polyoxyethylene ether (10) in aqueous solution', *J. Dispersion Sci. Technol.*, 2018, **39**, (8), pp. 1208–1213
[24] Wang N., Lin H., Zhao M., *ET AL.*: 'Spectroscopic studies of sodium dodecyl sulfate and Sudan red III associations in solutions', *AATCC J. Res.*, 2017, **4**, (4), pp. 16–21
[25] Goncharuk V.V., Bagrii V.A., Chebotareva R.D., *ET AL.*: 'Crystallization of calcium carbonate in magnetic water in the presence of paramagnetic substances', *Russ. J. Appl. Chem.*, 2008, **81**, (12), pp. 2108–2111
[26] Wang Z., Jing J., Wang D., *ET AL.*: 'Dye-surfactant solution of Coomassie Brilliant Blue G250 and tween 20: micellar and interaction parametric studies', *AATCC J. Res.*, 2019, **6**, (3), pp. 20–27
[27] Wang N., Lin H., Zhu H.: 'Study of the association behavior between bromophenol blue and octylphenol polyoxyethylene ether (10) in aqueous solution and the solubilization of bromophenol blue by micelles', *J. Solution Chem.*, 2016, **45**, (12), pp. 1689–1700
[28] Tang Y., Du B.Y., Li L.G., *ET AL.*: 'Effects of Tx-100-SDS on crystal growth of calcium carbonate in reverse microemulsion solution', *Chinese Sci. Bull.*, 2007, **52**, (1), pp. 78–83
[29] Chen D.H., Wu S.H.: 'Synthesis of nickel nanoparticles in water-in-oil microemulsions', *Chem. Mater.*, 2000, **12**, (5), pp. 1354–1360
[30] Cusack M., Freer A.: 'Biomineralization: elemental and organic influence in carbonate systems', *Chem. Rev.*, 2008, **108**, (11), pp. 4433–4454
[31] Nielsen M.H., Lee J.R.I., Hu Q., *ET AL.*: 'Structural evolution, formation pathways and energetic controls during template-directed nucleation of $CaCO_3$', *Faraday Discuss.*, 2012, **159**, pp. 105–121
[32] Aizenberg J., Black A.J., Whitesides G.M.: 'Control of crystal nucleation by patterned self-assembled monolayers', *Nature*, 1999, **398**, (6727), pp. 495–498
[33] Greer H.F., Zhou W., Guo L.: 'Phase transformation of Mg-calcite to aragonite in active-forming hot spring travertines', *Mineral. Petrol.*, 2015, **109**, (4), pp. 453–462
[34] Arriagada F.J.: 'Synthesis of nanosize silica in a nonionic water-in-oil microemulsion', *J. Colloid Interface Sci.*, 1999, **220**, pp. 210–220
[35] Hartman P., Perdok W.G.: 'On the relations between structure and morphology of crystals I', *Acta Crystallogr.*, 1955, **8**, (1), pp. 49–52
[36] Feldmann T., Demopoulos G.P.: 'The crystal growth kinetics of alpha calcium sulfate hemihydrate in concentrated $CaCl_2$-HCl solutions', *J. Cryst. Growth*, 2012, **351**, (1), pp. 9–18
[37] Li X., Hu Q., Yue L., *ET AL.*: 'Synthesis of size-controlled acid-resistant hybrid calcium carbonate microparticles as templates for fabricating 'micelles-enhanced' polyelectrolyte capsules by the LBL technique', *Chem. Eur. J.*, 2006, **12**, (22), pp. 5770–5778
[38] Trautz O.R.: 'Crystallographic studies of calcium carbonate phosphate', *Ann. N. Y. Acad. Sci.*, 1960, **85**, (1), pp. 145–160
[39] Walsh D., Lebeau B., Mann S.: 'Morphosynthesis of calcium carbonate (vaterite) microsponges', *Adv. Mater.*, 1999, **11**, (4), pp. 324–328
[40] Yang Z., Peng H., Wang W., *ET AL.*: 'Crystallization behavior of poly (ε-caprolactone)/layered double hydroxide nanocomposites', *J. Appl. Polym. Sci.*, 2010, **116**, (5), pp. 2658–2667
[41] Andersen F.A., Brečević L.: 'Infrared spectra of amorphous and crystalline calcium carbonate', *Acta Chem. Scand.*, 1991, **45**, pp. 1018–1024
[42] Greer H., Wheatley P.S., Ashbrook S.E., *ET AL.*: 'Early stage reversed crystal growth of zeolite A and its phase transformation to sodalite', *J. Am. Chem. Soc.*, 2009, **131**, (49), pp. 17986–17992
[43] Calvaruso G., Minore A., Liveri V.T.: 'FT-IR investigation of the urea state in AOT reversed micelles', *J. Colloid Interface Sci.*, 2001, **243**, (1), pp. 227–232
[44] Greer H.F., Yu F., Zhou W.: 'Early stages of non-classic crystal growth', *Sci. China: Chem.*, 2011, **54**, (12), pp. 1867–1876
[45] Chen S.F., Yu S.H., Wang T.X., *ET AL.*: 'Polymer-directed formation of unusual $CaCO_3$ pancakes with controlled surface structures', *Adv. Mater.*, 2005, **17**, (12), pp. 1461–1465
[46] Liu Z., Pan H., Zhu G., *ET AL.*: 'Realignment of nanocrystal aggregates into single crystals as a result of inherent surface stress', *Angew. Chem., Int. Ed.*, 2016, **55**, (41), pp. 12836–12840
[47] Chen X., Qiao M., Xie S., *ET AL.*: 'Self-construction of core-shell and hollow zeolite analcime lcositetrahedra: a reversed crystal growth process via oriented aggregation of nanocrystallites and recrystallization from surface to core', *J. Am. Chem. Soc.*, 2007, **129**, (43), pp. 13305–13312
[48] Ghaedamini H., Amiri M.C.: 'Effects of temperature and surfactant concentration on the structure and morphology of calcium carbonate nanoparticles synthesized in a colloidal gas aphrons system', *J. Mol. Liq.*, 2019, **282**, pp. 213–220
[49] Liveri V.: 'Reversed micelles as nanometer-size solvent media', in Rosoff M., [ED]: Nano-Surface Chemistry, (Marcel Dekker, USA, 2001) pp. 473–504
[50] Warr G.G., Sen R., Evans D.F., *ET AL.*: 'Microemulsion formation and phase behavior of dialkyldimethylammonium bromide surfactants', *J. Phys. Chem.*, 1988, **92**, (3), pp. 774–783